Etude No. 161
Projet N° 103
IGM85- 103-161

FRACTURE OF MICA-REINFORCED POLYPROPYLENE: MICA CONCENTRATION EFFECT

by

T. Vu-Khanh, B.Sanschagrin and B. Fisa
National Research Council Canada
Industrial Materials Research Institute
75, boul. De Mortagne
Boucherville, Québec J4B 6Y4

CNRC N° 23802

FRACTURE OF MICA-REINFORCED POLYPROPYLENE: MICA CONCENTRATION EFFECT

By

T. Vu-Khanh, B. Sanschagrin and B. Fisa
National Research Council Canada
Industrial Materials Research Institute
75, De Mortagne
Boucherville, Quebec J4B 6Y4

ABSTRACT

Concepts of post-yield fracture mechanics were used to characterize the crack initiation and propagation resistances of mica-reinforced polypropylene containing different mica concentrations. Although mica addition leads to an apparently brittle composite, the crack initiation resistance is slightly increased with mica concentration up to 10% by weight and significant improvement in crack propagation performance was found for polypropylene reinforced by up to 20% of mica in comparison to that of virgin polypropylene. The debonding of the interface between mica flakes and the matrix leads to a micro-ductility ahead of the crack tip in which the matrix is able to pull-out from mica particles and to stretch. This micro-ductility also prevents the brittle, unstable crack propagation which is due to the coalescence of voids in pure polypropylene. Above 20% of mica the reduction of the effective amount of the matrix material results in a substantial drop in the resistance to crack growth of mica-reinforced polypropylene.

INTRODUCTION

Fillers have been widely used in commercial production of polymers to improve physical properties for specific applications. The main effects of fillers on polymers are the increase of modulus and hardness, and the reduction of creep and distortion at elevated temperature (1). One of the recent additions to the family of fillers is ground and delaminated mica. This filler has been shown to be an attractive material since it combines interesting performance improvement with low cost. Addition of mica to plastics improves the chemical resistance and dimensional stability and reduces the gas diffusivity of the resulting composites (2, 3). According to the theoretical calculations of platelet reinforced composites (4, 5), the modulus of polymers reinforced by mica is, in general, significantly increased as shown in the case of mica-reinforced polypropylene (6-12).

However the effects of mica on polymer strength remain unclear. Although theoretically mica should substantially increase the strength of plastics (4, 5, 13), Okuno and Woodhams (7) and Boaira and Chaffey (8) have noted a drop in strength for mica-reinforced polypropylene in the absence of a coupling agent due to poor bonding between mica and polymer. When a coupling agent is used, strength performance can be moderately improved. On the other hand, the impact resistance of polymers, as measured by Charpy or Izod tests, deteriorates when mica is added (6, 9, 12, 13, 16). As pointed out by Friedrich and Karsch (15), when a thermoplastic polymer orientates or crystallizes with strain, it exhibits poor bonding with fillers. Consequently, it is able to separate and deform away from the filler surface (to stretch and to work harden). The matrix stretching generally requires a large amount of energy in a fracture process whereas the energy required for the formation of voids and cracking of the interface between the polymer and the filler is considerably smaller. For these reasons the addition of fillers usually results in a more or less continuous and drastic reduction of the fracture properties. A better understanding of the fracture resistance of mica-filled polypropylene is thus needed for a more confident use of this material.

In this study the fracture strength and mechanisms of a mica-reinforced homopolymer polypropylene were investigated. Fracture mechanics were used to characterize the material capacity to resist the crack growth. This type of study is very important because failure processes are very often associated with the propagation of cracks originating from flaws and that fracture resistance of polymers is related to its crack extension resistance. In linear elastic fracture mechanics the material parameters which characterize the crack initiation are described by the fracture toughness K_c or G_c (16-18). For a valid evaluation of these fracture toughness parameters, the theory envisages the dimensions of the specimen and the crack to be much larger than the size of the plastic zone around the crack tip. For ductile materials like plastics, a substantial amount of plasticity may occur before the crack starts to grow (19-21). This requires that the dimensions of the specimens used for the determination of G_c or K_c must be very large. However, injection molded products are relatively thin compared to the size of the plastic zone, invalidating the use of linear elastic fracture mechanics. In the case of large-scale plasticity, post-yield fracture mechanics such as the path independent J-integral and the crack growth resistance R-curve method must be used as a quantitative characterization of fracture toughness. The latter concepts were employed to examine the fracture processes of mica-reinforced polypropylene. The fracture parameters in the elastic-plastic regime are also discussed.

EXPERIMENTAL

Materials:

A phlogopite mica with a high aspect ratio, supplied by Marietta Resources International Ltd., Boucherville, Canada, was chosen for this study. This commercially available mica was an untreated Suzorite 200HK grade having a volume average flake diameter (22) of 149μm and a shape factor ψ of 59.1, the latter parameter being closely related to the average aspect ratio (22).

The polymer was an injection grade polypropylene, Profax 6301 from

Hercules Canada Ltd. The resin was in powder or "as polymerized" form, (with a melt index of 12 g/10 min. ASTM D1238) and an intrinsic viscosity of 1.7 (Decahydronaphthalene, 135°C).

Sample preparation:

Mica and polypropylene powders were dry blended in a Welex high intensity mixer (Model ESK-80) to obtain 1, 3, 5, 10, 20, 40 and 60 percent by weight of mica content. The dry blend was fed directly into an Engel reciprocating injection press (Model Es 150-70) having a clamping force of 70 tons.

The tensile-specimens (ASTM D638, type I) were molded using process conditions previously published (22). Samples for fracture tests (Fig.1) were made by machining away sides of injection molded plates (initial dimensions 6 X 30 X 90 mm).

Testing procedure:

All tests were performed on a standard testing machine (Instron, Model 1125). The tensile tests were performed with a cross-head speed of 10mm/min. The initial tangent modulus was determined from the slope of the load-deformation curves. The deformations were measured by a strain gage extensometer Instron, Model No. A325-24 2630-004, having a gage length of 1 inch. The yield strength was determined as the maximum load divided by the initial section of the specimen. An average value was determined from 6 samples.

The fracture toughness was measured, using the three-point-bend specimen, with a ratio of support span to specimen width, S/D, of 4 according to the recommendation of the ASTM standard test method, designation E-399.

The initial crack made in the three-point-bend specimen was 5.2 mm long, giving a ratio of initial crack length over specimen width (a/D) of 0.4. The initial crack was first made with a band saw to a depth of 3 mm and the final 2.2 mm was done by forcing a razor blade into the specimen in a special jig on a laboratory press. The notch made by the razor blade had

a radius of less than 30 μm.

The cross-head speed in the three-point-bend fracture toughness tests was also 10 mm/min.

RESULTS AND DISCUSSION

Preliminary results:

Figures 2 to 4 show the effects of mica content on the Young modulus, the yield strength and the yield and fracture elongations of mica-reinforced polypropylene. As pointed out in previously reported investigations, the Young modulus was found to increase strongly with mica content. The yield strength is slightly improved up to 10%; beyond 10% it decreases. However, the variation of the yield stress remains relatively small for all mica concentrations. This effect of mica on the yield strength of polypropylene is similar to its effect on low-density polyethylene (23)

In Fig. 4 the yield and fracture elongations are plotted against mica content. Since it is very difficult to measure the true deformation at necking point, these elongations are considered to be the nominal deformations of the specimen gage length at yield and fracture. The nominal yield and fracture elongations are considerably reduced when mica is added (Fig. 4). These results suggest that mica addition would lead to a more or less continuous and drastic reduction of the fracture properties, resulting in a brittle product as is the case in other filled polymers.

However, the load-displacement curves of the fracture toughness tests (Fig. 5) on three-point-bend specimens show a surprising effect. In the presence of a sharp notch, virgin polypropylene exhibits a purely brittle behavior. Fracture occurs at a constant deflection with the aid of the energy provided by the elastic strain energy stored in the sample. With the addition of mica the fracture behavior of mica-reinforced polypropylene becomes more and more ductile. Up to 5% by weight of mica the unstable fracture (at constant displacement) still occurs but the amounts

of plastic deformation and stable crack growth are increased with mica content. The plastic deformation accompanied by stable crack propagation is represented by the non-linear region of the load versus displacement curve. Since the area under these curves increases, the energy absorbed by the specimen to fracture increases with mica content, all the specimens tested having the same crack length and dimensions. Above 5% no unstable fracture was observed at the cross-head speed of 10 mm/min. The crack grows with continuous supply of energy from the external load (with continuous increase in displacement until complete fracture). The amount of energy absorbed by the specimen to break which is represented by the area under the load deflection curve continues to augment up to 20% mica . Above 20%, the stable fracture still occurs but the area under the load deflection curve decreases as the mica content is increased. This shows a diminution of the energy absorbed by the specimen.

The plane strain fracture toughness testing requires a small-scale yielding condition, that is, the crack length, specimen thickness and the specimen width must be much larger than the plastic zone size at the crack tip (r_p). Based on Irwin's approximation of the radius of the plane strain plastic zone size:

$$r_p = \frac{1}{6\Pi} (K_{Ic}/\sigma_y)^2 \qquad [1]$$

where K_{Ic} is the material fracture toughness and σ_y is the yield stress. The criteria of validity of K_{Ic} value recommended in the standard procedure ASTM E-399 are:

$$\text{crack length } a > 2.5\ (K_{Ic}/\sigma_y)^2$$
$$\text{specimen thickness } B > 2.5\ (K_{Ic}/\sigma_y)^2$$

It is also required that the ratio of the maximum load (Pmax) to the load obtained from a secant offset P_q (see Ref. 21) must be less or equal to 1.1. These conditions are not satisfied in these fracture tests and the plane strain fracture toughness values determined from these curves

become meaningless. In this case the standard procedure recommends the use of a dimensionless value, the specimen strength ratio, as a comparative measure of the toughness. The specimen strength ratio of three-point-bend specimens is given by (24):

$$Rsb = 6\ Pmax\ D/B(D-a)^2\ \sigma_y \qquad [2]$$

It has also been shown that $\underline{Rsb}^2$ is proportional to $\underline{K_{Ic}^2/\sigma_y^2 D}$ (25) in the case of metals.

Figure 6 shows the variation of $\underline{Rsb}^2$ with mica content. This result indicates qualitatively that the plane strain fracture toughness of polypropylene increases with mica addition up to 20% by weight and decreases above this concentration. However the specimen strength ratio is only of comparative value and its relation to the plane strain fracture toughness in the case of composite materials has not yet been demonstrated because of the complexity of the fracture mechanisms of these materials (debonding between mica and matrix, formation of voids, matrix stretching, etc.). In order to confirm the effect of mica on crack initiation resistance of mica-reinforced polypropylene, other methods taking into account the plasticity at the crack tip must be used.

Crack initiation study:

In large scale plasticity, it has been shown that the stress and strain fields at the crack tip can be described with the aid of a contour integral commonly known as J-integral originated by Rice (26). It is defined for two-dimensional problems and is given by:

$$J = \int_\Gamma W dy - T \frac{\delta u}{\partial x}\ ds \qquad [3]$$

where Γ is any contour surrounding the crack tip, T is the traction vector defined by the outward normal $\underline{n}$ along Γ (Fig. 7), $T_i = \sigma_{ij}\ \underline{nj}$, s is the arc length along Γ, $\underline{u}$ is the displacement vector and $\underline{W}$ is the strain energy given by:

$$W = \int_0^{\varepsilon_{mn}} \sigma_{ij}\, d\varepsilon_{ij} \qquad [4]$$

Hutchinson (27) and Rice and Rosengren (28) have shown that a singularity does exist at the crack tip in large scale plasticity and the crack tip stress-strain singularity can be characterized by the J-integral parameter. It can therefore be used as a failure criterion for large scale yielding. J also represents the flow of energy into the crack tip region and is stated mathematically as:

$$J = -\frac{dU}{da} \qquad [5]$$

where U is the potential energy and a is the crack length (27). For the pure elastic case (small scale yielding), the J-integral has been shown to be identical to the strain energy release rate G.

It is worth noting that as a fracture parameter, the J-integral has many limitations (29 31) and especially in the case of composite systems the deformation theory of plasticity is not applicable. In addition, there is formation of voids at the matrix-filler interface. This will result in a destruction of any characteristic crack tip singularity. However J can be considered as an alternative energy balance criterion of fracture since it represents the flow of energy into the crack tip region . Rice et al (32) have introduced an approximate equation for the calculation of J in deeply notched, bend-type specimens.

$$J = \frac{2U}{B(D-a)} \qquad [6]$$

where U is measured from the area under the load versus load point deflection curve. This equation is the basis for the multiple specimen resistance (R) curve method for determining the fracture toughness first developed by Landes and Begley (33) which is now the ASTM recommended standard procedure (34). This method consists of loading several identical specimens having the same initial crack length to different

values of load point deflection and then unloading. These specimens will thus exhibit different amounts of crack growth. After unloading, the crack advance is marked by a penetrant ink and the specimen is broken open by impact at room temperature. The value of J at the point where the specimen is unloaded is determined from Eq. (6) for each specimen. This value of J is plotted as a function of crack advance (Δa). This gives the crack growth resistance curve from which the fracture toughness at crack initiation J_{Ic} is determined at the intersection of the blunting line and the straight line fitted to the crack growth resistance curve as illustrated in Fig.8.

Figure 9 shows the J versus Δa curves for different mica contents. The blunting lines based on $J=2\sigma_y \Delta a$ are also shown. It can be seen that the crack growth resistance is the same for 3, 5 and 10% by weight of mica when the crack advances. However, as pointed out previously, the amount of stable crack growth is lower with lower mica content. Above 10%, the crack growth resistance of mica-reinforced polypropylene decreases.

Figure 10 shows the fracture toughness at crack initiation for various mica concentrations. The J_{Ic} value increases at very low mica contents ($< 3\%$ by weight), and attains a plateau region between 3 and 10%. Beyond 10%, J_{Ic} decreases slightly up to 20% and then drastically between 20 and 40%. This result confirms the measured value of specimen strength ratio shown above (Fig. 6) except for 20% by weight of mica content. The maximum specimen strength ratio was found for samples containing between 3 and 20% mica. On the other hand, the J-integral study shows that the plane strain fracture toughness at crack initiation decreases above 10%. This suggests that at maximum load, there is probably a certain amount of stable crack growth which has already occurred, accompanied by an increase in the crack growth resistance. The maximum load may then not be an indication of the plane strain fracture toughness in this particular case. The effect of mica on the fracture toughness of mica-reinforced polypropylene is also rather surprising compared to the appearance of the load-deformation curves of fracture. These curves

indicate a much more pronounced effect of plasticity when mica is added, resulting in a higher energy required to break the specimen. It can be concluded from these results that addition of mica has a more pronounced effect on the crack propagation processes than on the crack initiation resistance.

The J-integral (R) curve method is not valid however for crack growth study. In this method no crack growth is permitted because it necessarily involves unloading. This requires that the amounts of crack growth permitted in the multiple specimen resistance (R) curve method for determining J_{Ic} must be insignificant. The J_{Ic} fracture criterion refers to crack initiation rather than propagation.

Crack propagation study:

Theoretically, in order that a crack can propagate, the energy available for crack propagation must be higher than or equal to the fracture energy of the material. The energy available for crack propagation or the strain energy release rate of a three-point-bend specimen can be calculated with the aid of the calibration factor used in the calculation of the stress intensity factor as discussed in Ref. (35). The energy balance of a loaded specimen containing a crack shows that the strain energy release rate can be expressed as follows:

$$G = -\frac{1}{2} P^2 \frac{dC}{dA} = \frac{1}{2} \frac{\Delta^2}{C^2} \frac{dC}{dA} \qquad [7]$$

where P is the applied load, C is the specimen compliance, Δ is the load point deflection and A is the crack area. C and dC/dA can be calculated numerically as shown in the Appendix. G can then be determined from Eq. [7]. Figure 11 shows the variation of the dimensionless value of the strain energy release rate GD/E versus the crack length for different deformation levels in a three-point-bend specimen having a ratio of support span to specimen width of 4. The conditions for stable and unstable

crack propagation are also illustrated in Figure 11 and have been thoroughly discussed in Ref. (35). For a material having a constant fracture energy during crack propagation, the crack can propagate in a stable or in an unstable manner depending on its initial length. For crack lengths shorter than $(a/D)_{lim}$, the crack will propagate in an unstable manner since the energy release rate of the specimen increases for a constant deformation when the crack advances. For crack lengths $a/D \geq (a/D)_{lim}$, this energy release rate decreases with crack growth and the crack can propagate only if additional energy is provided, i.e. when the deformation is increased. In this case the crack propagation is stable.

Fig. 11 shows that the value of $(a/D)_{lim}$ is about 0.35. All the tested specimens were thus in a stable fracture condition with an initial crack length of 0.4. The fact that brittle fracture occurs in virgin polypropylene and at low mica content is probably due to the blunting effect in which the hydrostatic stress component reaches a critical value at a certain distance ahead of the crack tip. The blunting-induced unstable fracture is a phenomenon often observed in polymers where a fracture nucleus forms ahead of the crack tip as in the case of polycarbonate (36) and polyamide 11 (35, 37). For polypropylene, the fracture nucleus was believed to be related to the craze formation (38). This fracture mechanism will be further discussed later. According to the shape of the available energy for the crack propagation curve for long cracks (Fig. 11), after instability the fracture energy should decrease considerably in order to satisfy the energy balance condition $G > Gc$. Thus the addition of mica improves the crack growth resistance of polypropylene in preventing brittle fracture, even though the crack growth resistance (J_{Ic}) at crack initiation is not significantly affected.

The fracture energy during crack propagation can be characterized by calculating the variation of the critical stress intensity factor during crack extension. This variation is also called the crack growth resistance curve or R-curve (39). It has been shown that there is a unique

relationship between the amount of crack extension and the applied stress intensity factor for a given thickness. R-curve is often used to characterize the crack growth resistance of materials in which plastic deformation is large and as the the crack grows, the resistance to fracture increases due to the increased volume of plastically deformed material ahead of the crack tip. The R-curve is now an ASTM standard procedure (40) for Center-Cracked Tension panel (CCT), Compact Specimen (CS) and the Crack-Line-Wedge-Loaded specimen (CLWL). For three-point-bend specimens the determination of the variation of the critical stress intensity factor with crack extension requires the determination of the specimen compliance versus the crack length. The compliance calculation and R-curve determination are given in the Appendix.

Figure 12 shows R-curves for various mica contents. The crack extension resistance K_R is plotted against the effective crack length determined by the secant method (see Appendix), the effective crack length being the physical crack size augmented for the effects of crack tip plastic deformation. The modulus used for the calculation of the effective crack length $a_{eff.}$ was the effective modulus determined from the initial slope of the load-displacement trace as discussed in Ref. (41). Figure 12 shows that for up to 10% by weight of mica the crack extension resistance (K_R) increases at a constant rate when the crack is growing and that the amount of stable crack propagation before brittle fracture increases with mica content. At 10% no brittle fracture was observed; fracture was completely stable over the entire broken surface and a plateau region was observed at maximum value of K_R. At 20% mica content K_R is less than that at 10% in the early stage of crack extension (Fig. 13) but attains a higher plateau region (at maximum K_R value). Above 20% of mica concentration the fracture resistance is considerably reduced on the entire R-curve.

These results show that although mica addition leads to an apparently brittle composite by reducing both the yield strength and the fracture elongation of the material, in the presence of a defect (crack), the presence of mica can augment the ductility locally, resulting in a higher

fracture energy (higher K_R value) during crack propagation of polypropylene reinforced by up to 20% of mica. The fracture energy at crack initiation, as shown in J_{Ic} measurement, is also slightly improved up to 10% by weight of mica content. At 20%, the fracture energy at crack initiation decreases slightly but the maximum fracture energy attained in this case is much higher. Figure 14 shows the maximum critical stress intensity factor reached during crack extension for various mica contents. This demonstrates the considerable enhancement of fracture resistance of polypropylene when it is reinforced by up to 20% of mica. Moreover, mica addition can prevent unstable crack propagation which is the cause of most catastrophic failures. It is worth noting that this effect of mica on fracture resistance would be expected to be more important for materials which exhibit strong notch sensitivity as in the case of polypropylene. This material is normally very ductile with a high capacity for stretching, but in the presence of a crack the hydrostatic component of stress ahead of the crack tip leads to craze formation and, when the voids in the craze region coalesce, they cause catastrophic fracture. The effect of mica in this case is to permit the matrix to pull out and to stretch as illustrated in Fig. 15, giving a higher crack tip opening displacement (δ_c) and a higher crack growth resistance since these parameters have been shown to be directly related by:

$$K_c^2 = mE\sigma_y\delta_c$$

where m is a constant. This effect will be further demonstrated by microscopic examination of the fracture surfaces.

Fractographic examination

Figure 16 shows the micrograph, as viewed by the scanning electron microscope, of the fracture surface of virgin polypropylene and Fig. 17 shows this surface in the region just ahead of the notch tip. In the blunting region there are circular marks of void formation and growth as

shown, at a higher magnification, in Figure 18. The size of circular marks seem to decrease when the distance from the notch tip increases. This is probably due to a higher density of void nucleation since the triaxiality of stress rises to a maximum at a certain distance from the notch tip. The circles in Fig. 16 and 17 indicate the region where a fracture nucleus is formed, leading to a brittle fracture. This fracture nucleus is probably associated with the coalescence of voids in the region of maximum hydrostatic component of stress since in this region the density of voids and their growth rate would be expected to be the highest.

Figure 19 shows the fracture surface of polypropylene reinforced with 3, 5, 10, 20 and 60% by weight of mica. These fracture surfaces reveal a greater local ductility than that of pure polypropylene. The micro-drawing of the matrix is more pronounced when mica content is increased. Since the crack growth resistance of mica-reinforced polypropylene is improved with the addition of mica, at least up to 20% of mica concentration, the micro-drawing observed on the fracture surface should be the cause of the improved fracture resistance . The matrix drawing can also be attributed to the debonding between mica flakes and the matrix. It can be seen on these fracture surfaces that in general the matrix is pulled out from mica particles and the stretching effect of the matrix is mainly around these mica flakes.

At low mica levels (Fig. 19a-19c) void formation can be seen in the matrix between the stretching regions and seems also to diminish as the mica content is increased. Since void coalescence is responsible for unstable, brittle fracture in virgin polypropylene, the void reduction is probably the cause of an increase in the amount of stable crack growth preceding unstable fracture when the mica fraction is increased. At 10% of mica the voiding effect seems to be at a minimum and at 20%, no void formation was observed on the fracture surface. This observation explains the disappearance of unstable fracture above 5% mica concentration.

At this stage it is not clear why the fracture energy at crack initiation

and the crack growth resistance during stable crack propagation are identical for mica content of 3 to 10% even though the stretching effect seems to increase and voiding seems to decrease. The only explanation proposed for the moment is that the debonding between the matrix and mica particles occurs probably very early with a very small interfacial fracture energy and the matrix acts alone to bear the load and to resist the crack propagation. From the relationship $\underline{K_R}^2 = \underline{m}\varepsilon_y\underline{E}\delta_c$, the crack opening displacement δ_c should increase with mica content according to an observed increase of drawing. The local yield elongation remains constant but since the effective section of the matrix decreases with higher mica content, $\underline{E}$ would decrease and $\underline{K_R}$ remain the same for mica content from 3 to 10% by weight.

Above 20% mica, the maximum drawing of the matrix is attained, but since the effective amount of the matrix material is small, as can be seen in Fig. 19e for the case of 60% of mica, the energy dissipated in plastic deformation of the matrix is reduced resulting in a decrease of the fracture energy of the composite.

SUMMARY AND CONCLUSION

When polypropylene is reinforced by mica the modulus is increased and the yield stress is slightly decreased. The yield and fracture elongations are also considerably reduced leading to an apparently brittle material. However in the presence of a defect, such as a crack, pure polypropylene breaks in a very brittle manner with low fracture energy due to the formation of voids in the crazed region ahead of the crack tip. This fracture behavior of polypropylene is much improved by the addition of up to 20% mica. In the presence of mica particles, the debonding between the matrix and mica flakes, which requires very little energy, causes a shear yielding deformation and a stretching effect of the matrix. This matrix drawing prevents the coalescence of voids, which normally occurs in the craze region of polypropylene and causes catastrophic failure.

Micro ductility induced by mica leads to a greater fracture energy at crack initiation for mica levels of up to 10% by weight. In this range, the amount of stable crack growth preceding the brittle fracture is also increased substantially accompanied by a reduction of the voiding effect in the matrix. The unstable fracture, which is due to the blunting effect at the crack tip was not observed at mica concentration of 10% and more. During the stable crack propagation, the crack growth resistance also increases strongly with crack extension and attains a maximum plateau value in the case of complete stable fracture. In polypropylene containing more than 10% of mica by weight the fracture energy at crack initiation decreased. The rate of decrease of J_{Ic} is greatest between 20 and 40% mica. At levels of 10 to 20% and above 40% J_{Ic} decreases only moderately with the increasing mica content. J_{Ic} above 40% of mica is five times less than that observed below 20% mica loading.

At 20% of mica the crack growth resistance is reduced compared to that at lesser mica concentration in the early stage of crack extension. However the resistance to crack propagation increased strongly during crack extension and attains a higher maximum value. At concentrations higher than 20% the maximum crack extension resistance decreased with the increasing mica content although the brittle (unstable) fracture was not observed. This was probably due to the reduction of the remaining matrix material resisting crack extension, even though maximum local deformation of the matrix was apparent.

Current work on this subject is focussed on the effect of other variables such as flake size, surface treatment and flake orientation on the fracture behavior of mica-reinforced polypropylenes.

ACKNOWLEDGEMENT

The authors would like to express their thanks to Mr J. Dufour and to Mr. M. Thibodeau for their help in performing the experimental part of this investigation.

LIST OF SYMBOLS

a	crack length
A	crack surface area
Δa	crack extension
B	specimen thickness
C	specimen compliance
D	specimen width
E	Young modulus
$f(a/D)$	geometric correction factor for K determination
G	strain energy release rate
G_c	fracture energy
J	contour integral
J_{Ic}	critical J value at crack initiation (toughness parameter)
K	stress intensity factor
K_c	fracture toughness (critical stress intensity factor)
K_R	critical stress intensity factor during crack propagation
P	load
$P_{max.}$	maximum load
P^e	load determined by the secant offset
R_{sb}	specimen strength ratio
S	specimen span
T	traction vector
u	displacement vector
W	strain energy
δ_c	crack opening displacement
ε	strain
σ	stress
Δ	load point deflection

REFERENCES

(1) M.O.W. Richardson, "Polymer Engineering Composites", Applied Science Publishers Ltd., London (1977).

(2) R.T. Woodhams and M. Xanthos, "Handbook of Fillers and Reinforcements for Plastics", H.S. Katz, J.V. Milewski Eds., p. 333, Van Nostrand Reinhold Co., New York (1978).

(3) M. Xanthos, Plast. Comp., 2 (4), 19 (1979).

(4) G.E. Padawer and N. Beecher, Polym. Eng. Sci., 10 185 (1970).

(5) M.R. Piggott, J. Mat. Sci., 8, 1373 (1973).

(6) J. Lusis, R.T. Woodhams and M. Xanthos, Polym. Eng. Sci., 13, 139 (1973).

(7) K. Okuno and R.T. Woodhams, Polym. Eng. Sci., 15, 308 (1975).

(8) M.S. Boaira and C.E. Chaffey, Polym. Eng. Sci, 17, 715 (1977).

(9) S.E. Tausz and C.E. Chaffey, J. Appl. Polym. Sci., 27, 4493 (1982).

(10) J.P. Trotignon, B. Sanschagrin and Piperaud, J.Verdu, Polym. Compos., 3, 230 (1982).

(11) C. Busigin, G.M. Martinez and R.T. Woodhams, Polym. Eng. Sci., 23, 766 (1983).

(12) C. Busigin, R. Lahtinen, G.M. Martinez, G. Thomas and R.T. Woodhams, Polym. Eng. Sci., 24, 169 (1984).

(13) F.W. Maine and P.D. Shepherd, Composites, 5 , 193 (1974).

(14) M. Fenton and G. Hawley, Polym. Compos., 3, 218 (1982).

(15) K. Friedrich, U.A. Karsch, J. Mater. Sci., 16, 2167 (1981).

(16) H. Liebowitz (ed.), "Fracture", Academic Press, New York (1968).

(17) J.F. Knott, "Fundamentals of Fracture Mechanics", Butterworth, London (1973).

(18) D. Francois, L. Joly, "La Rupture des Métaux", Masson et Cie, Paris (1972).

(19) P.L. Fernando and J.G. Williams, Polym. Eng. Sci., 20, 215 (1980).

(20) M.K.V. Chan and J.G. Williams, Polym. Eng. Sci., 21, 1919 (1981).

(21) M.K.V. Chan and J.G. Williams, Int. J. Fract., 145 (1983).

(22) B. Sanschagrin, B. Fisa, and B. Favis, Proc. SPE 42nd ANTEC, p. 683 (April 30 - May 3, 1984).

(23) M. Arina, A. Honkanen and V. Tammela, Polym. Eng. Sci, 19, 30 (1979).

(24) E 399 Standard Test Method for Plane Strain Fracture Toughness of Metallic Material, Annual Book of ASTM Standards.

(25) G. Succop, W.F. Brown Jr., ASTM STP632, 179 (1977).

(26) J.R. Rice, J. Appl. Mech., Trans. ASME, 379, June (1968).

(27) J.W. Hutchinson, J. Mech. Phys. Sol, 16, 13 (1968).

(28) J.R. Rice and G.F. Rosengren, J. Mech. Phys. Sol., 16, 13 (1968).

(29) J.A. Begley and J.D. Landes, ASTM STP514, part II, 1 (1972).

(30) J.D.G. Sumpter, C.E. Turner, ASTM STP601, 3 (1976).

(31) G.G. Chell, Ed., "Developments in Fracture Mechanics - 2", Applied Science Publishers, London, U.K., (1981).

(32) J.R. Rice, P.C. Paris and J.G. Merkle, ASTM STP536, 231 (1973).

(33) J.D. Landes and J.A. Begley, ASTM STP560, 170 (1974).

(34) E813 Standard Test Method for J_{Ic}, a Measure of Fracture Toughness, Annual Book of ASTM Standards.

(35) T. Vu-Khanh and F.X. de Charentenay, Polym. Eng. Sci., in press.

(36) M. Kitagawa, J. Mater. Sci., 17, 2514 (1982).

(37) F.X. de Charentenay, J.J. Robin, T. Vu-Khanh, 5th Int. Conf. on Deformation Yield and Fracture of Polymers, Cambridge, England, p. 33.1 (March 29 - April 1, 1982).

(38) M. Kitagawa and Yammaura, J. Mater. Sci., 19, 1863 (1984).

(39) R.H. Heyer, ASTM STP527, 3 (1973).

(40) E561 Standard Practice for R-Curve Determination, Annual Book of ASTM Standards.

(41) D.E. McCabe and J.D. Landes, ASTM STP668, 288 (1979).

APPENDIX

The stress intensity factor for a three-point-bend specimen is given (21) by:

$$K = (PS/BD^{3/2})\, f(a/D) \qquad [9]$$

where $f(a/D)$ is a calibration factor provided in Ref. (24). The strain energy release rate is expressed as (17)

$$G = \frac{K^2}{E} = \frac{1}{2} P^2 \frac{dC}{dA} = \frac{1}{2} \frac{\Delta^2}{C^2} \frac{dC}{dA}$$

Then, combining [9] and [10] dC/dA and C can be written as a function of a/D as follows:

$$\frac{dC}{dA} = \frac{dC}{d(a/D)BD} = \frac{S^2 [f(a/D)]^2}{EB^2D^3} \qquad [11]$$

$$C = C_o + \frac{1}{EB} \frac{S^2}{D} \int_o^{a/D} [f(a/D)]^2 \, d(a/D) \qquad [12]$$

where C_o is the specimen compliance for $a/D = 0$. By numerically calculating dC/dA and C, the available energy for crack extension, G, in a three-point-bend specimen can be obtained from Eq. [10] as a function of crack length a/D at different values of deformation Δ.

Knowing the relationship between the specimen compliance and the crack length, the effective crack length at any load level P can be determined as illustrated in Fig. 20.

FIGURE CAPTIONS

Figure 1 : Three-point-bend specimen used in fracture tests.

Figure 2 : Young modulus of mica-reinforced polypropylene as a function of mica concentration (wih cross-head speed of 10 mm/min.).

Figure 3 : Yield strength of mica-reinforced polypropylene as a function of mica concentration (with cross-head speed of 10 mm/min.).

Figure 4 : Yield and fracture elongations of mica-reinforced polypropylene as a function of mica concentration (with cross-head speed of 10 mm/min.).

Figure 5 : Schematic drawing showing load-deflection curves of the three-point-bending fracture tests at different mica concentrations. X represents the point at unstable, brittle fracture.

Figure 6 : Square of the specimen strength ratio ($\underline{Rsb^2}$) as a function of mica concentration.

Figure 7 : Crack tip coordinate system and arbitrary line integral contour.

Figure 8 : Procedure for $\underline{J_{Ic}}$ measurement.

Figure 9 : $\underline{J}$ versus crack extension for various mica concentrations.

Figure 10: Crack initiation resistance ($\underline{J_{Ic}}$) as a function of mica concentration.

Figure 11: Strain energy release rate in three-point-bend specimen versus crack length at different values of deflection.

Figure 12: Crack growth resistance (K_R) versus effective crack extension ($\Delta a_{eff.}$) at various mica concentrations.

Figure 13: Crack growth resistance (K_R) versus effective crack extension ($\Delta a_{eff.}$) for 3, 5, 10 and 20% of mica.

Figure 14: Maximum crack growth resistance attained as a function of mica concentration.

Figure 15: Schematic drawing of pull-out and stretching processes of the matrix ahead of the crack tip.

Figure 16: Micrograph of fracture surface of virgin polypropylene as viewed by scanning electron microscope.

Figure 17: Micrograph showing the fracture surface of virgin polypropylene in the region just ahead of the razor-notch tip.

Figure 18: Micrograph showing void formation and growth in the blunting region of virgin polypropylene.

Figure 19: Fracture surface of polypropylene reinforced by: 3%(a), 5%(b), 10%(c), 20%(d) and 60%(e) by weight of mica.

Figure 20: Schematic drawing of effective crack length determination from the load-deflection curve.

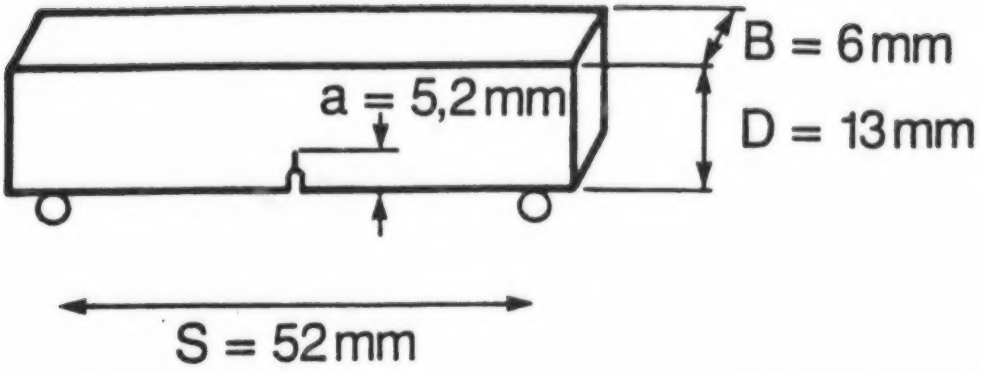

VU - KHANH

Fig. 1

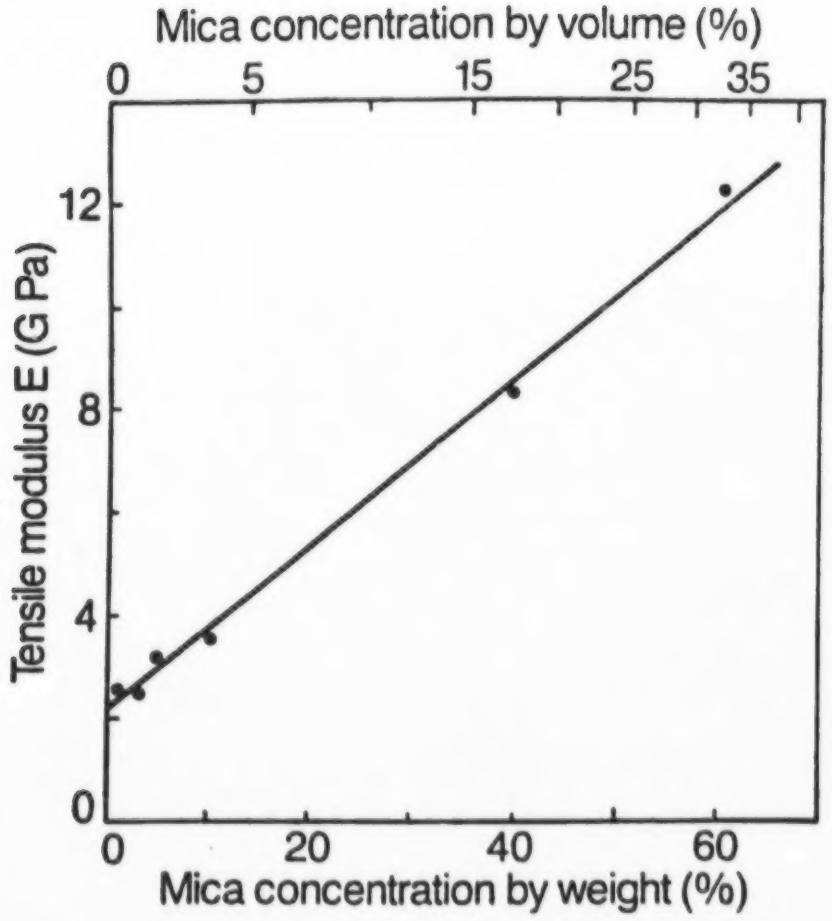
Mica concentration by volume (%)
0
5
15
25
35
Tensile modulus E (G Pa)
12
8
4
0
0
20
40
60
Mica concentration by weight (%)

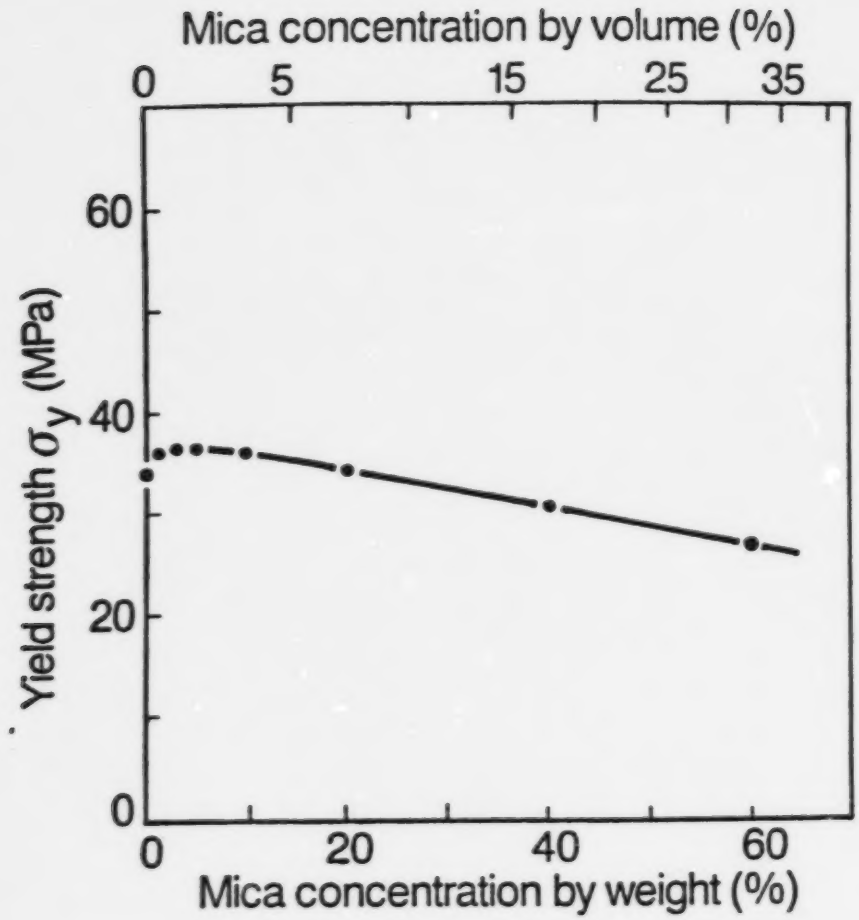

VU.KHANH Fig. 3

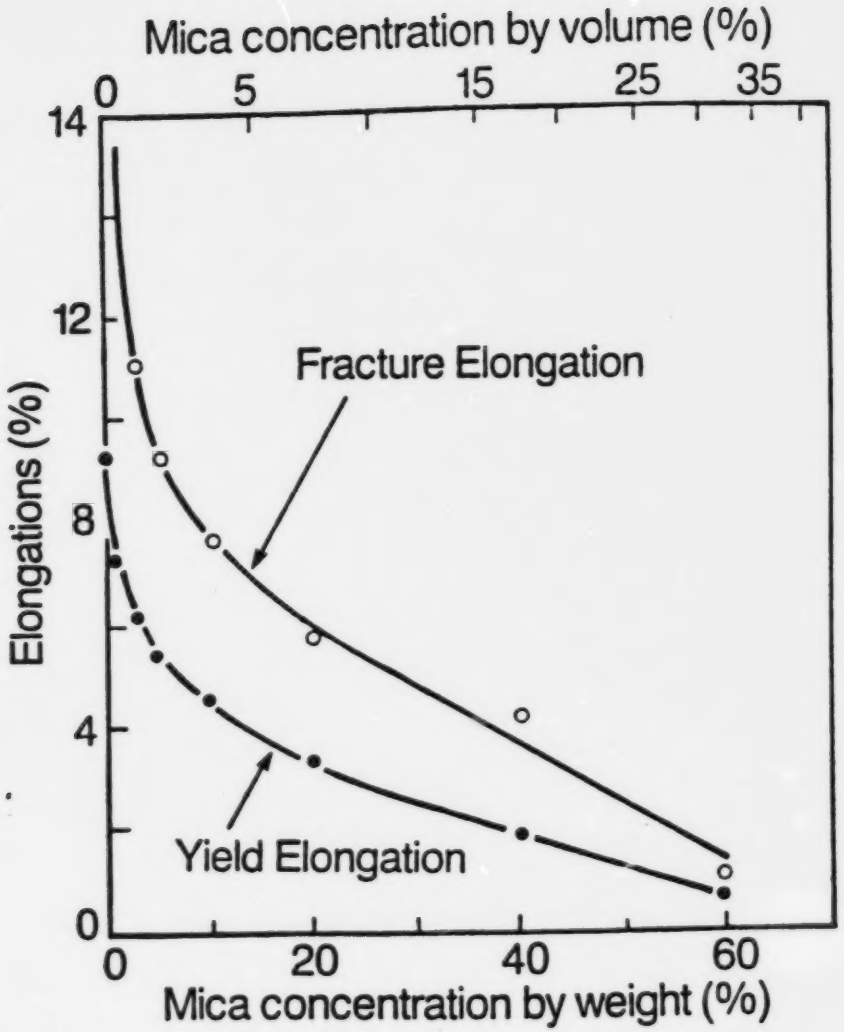

VU-KHANH Fig. 4

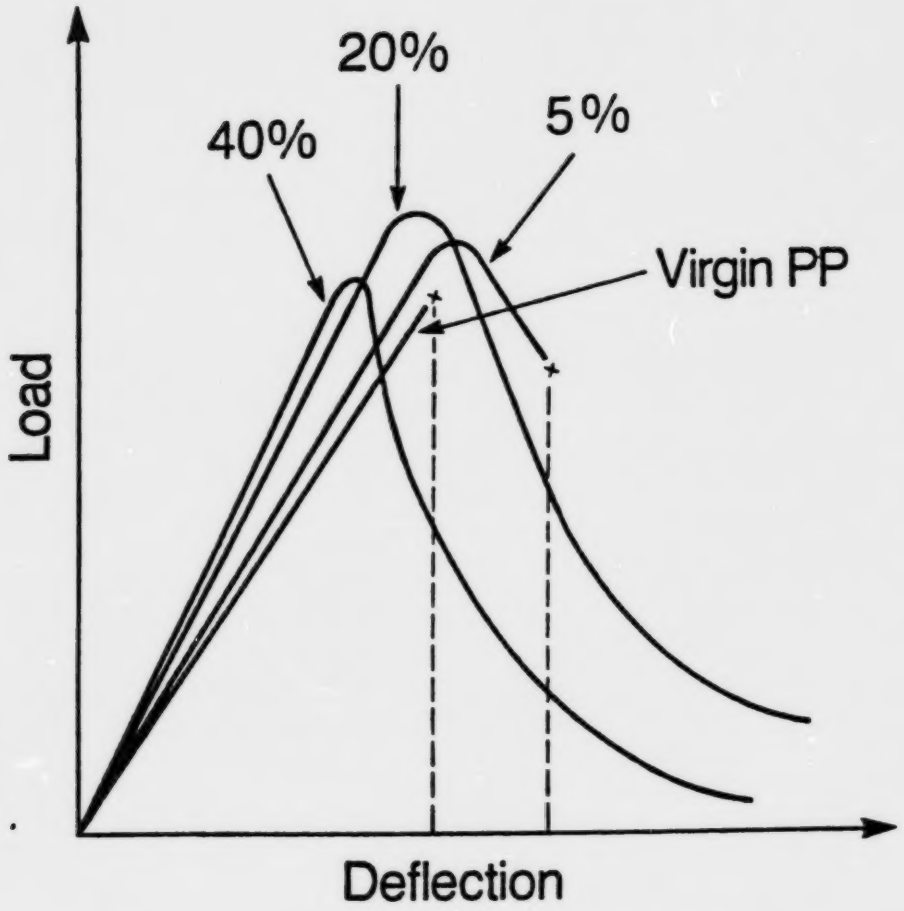

VU. KHANH Fig. 5

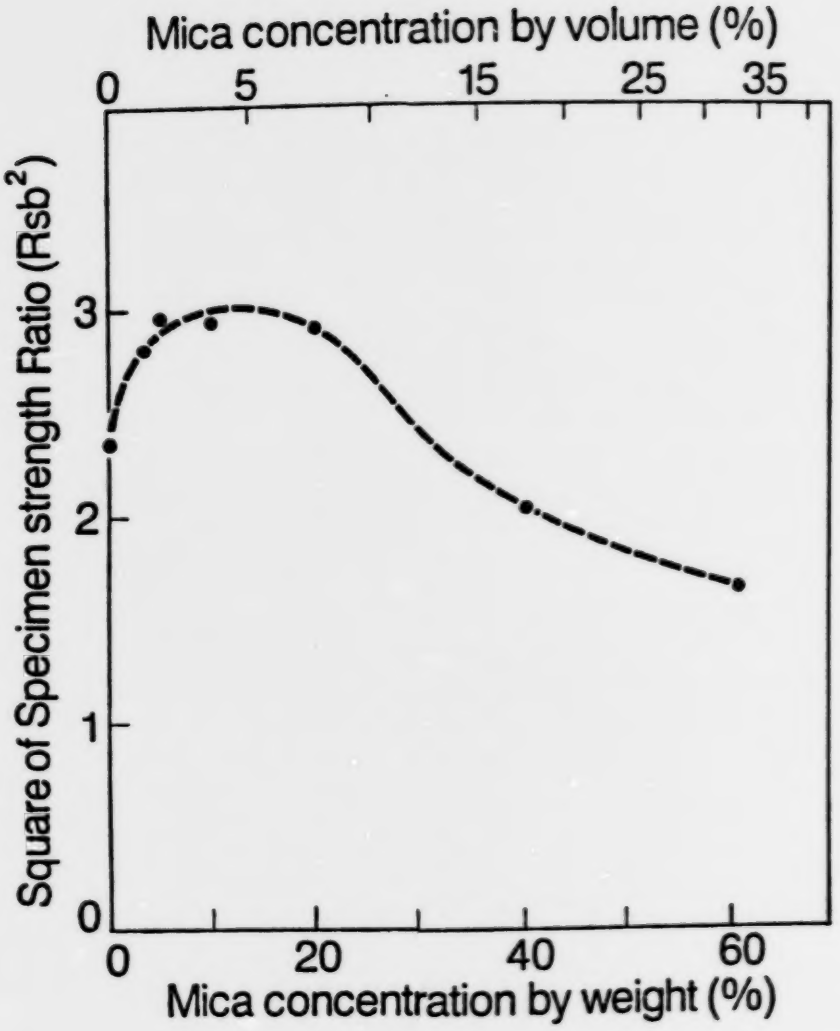

VU. KHANH Fig. 6

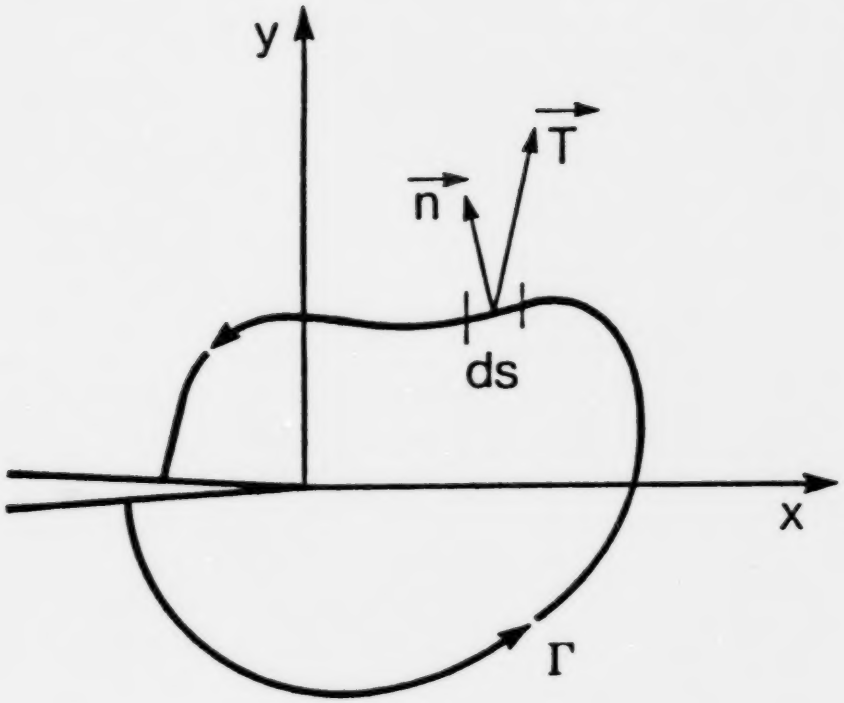

VU-KHANH Fig. 2

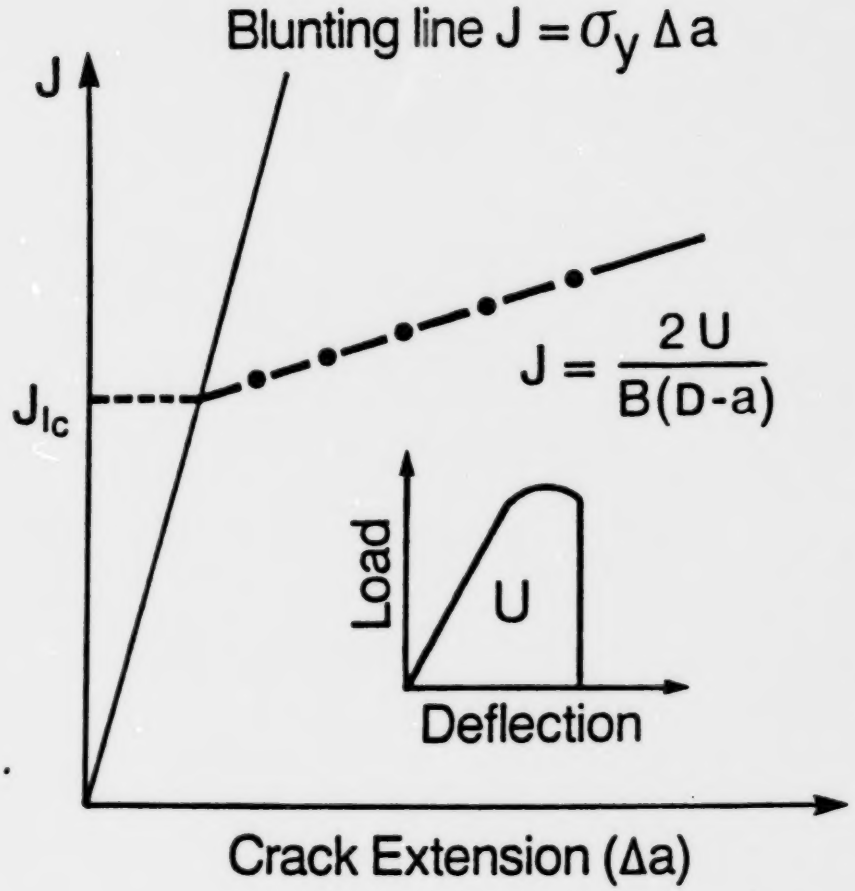

VIJ. KHANH Fig. 8

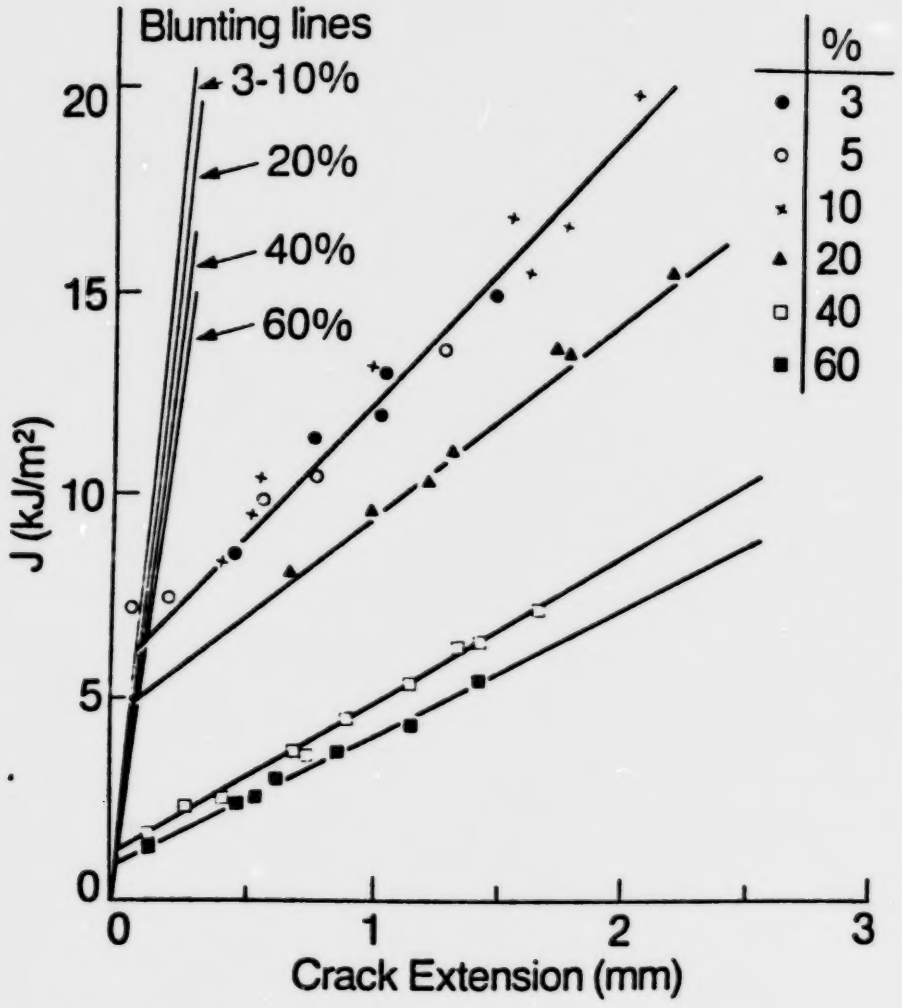

VU-KHANH Fig. 9

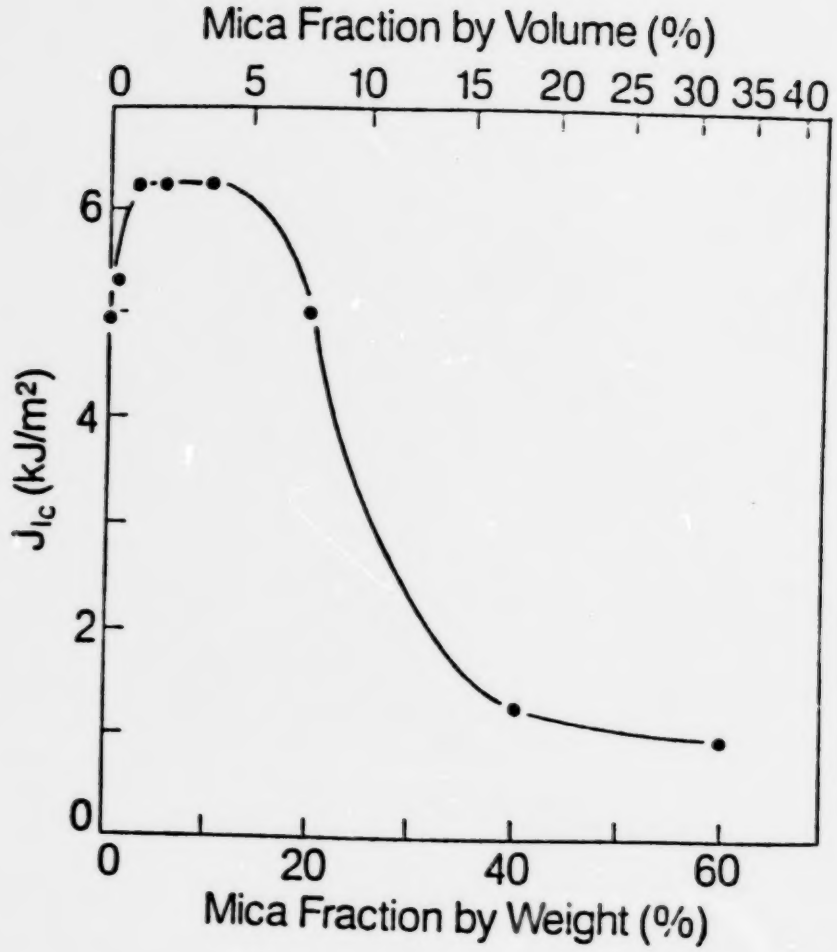

VU-KHANH Fig. 10

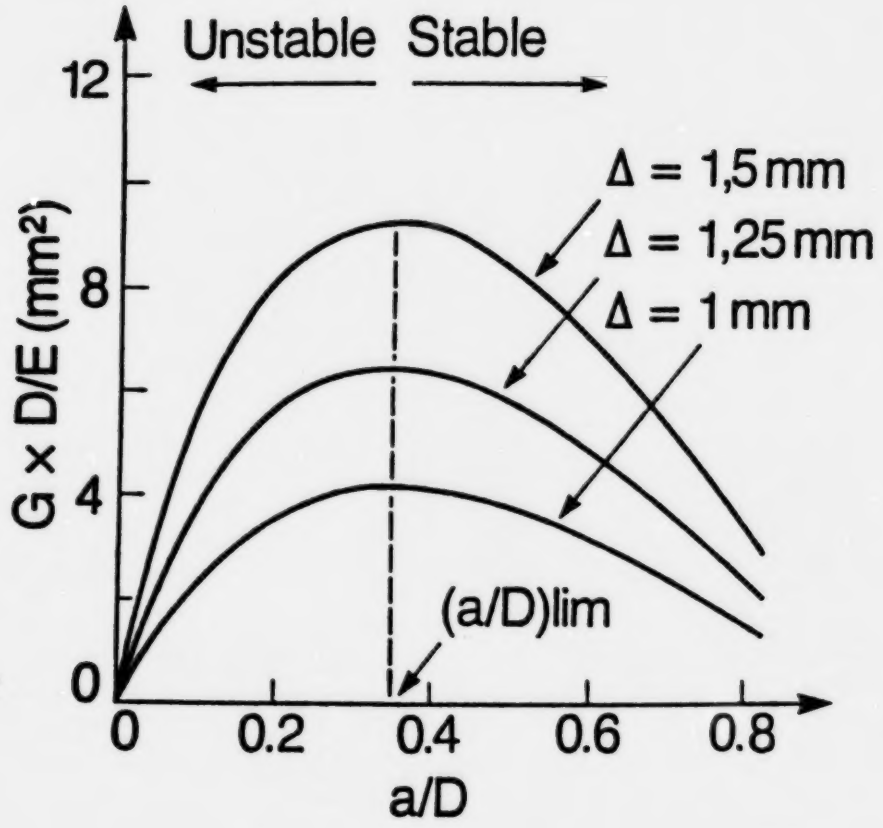

VU-KHANH Fig. 11

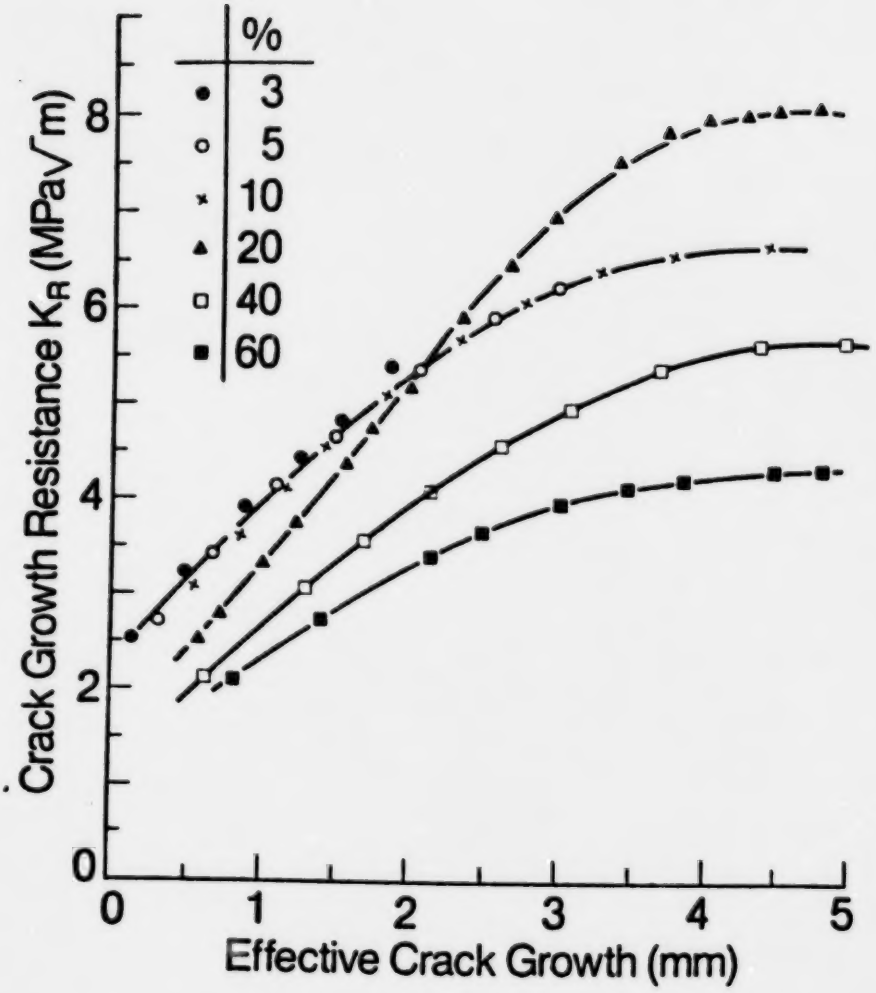

VU KHANH Fig. 12

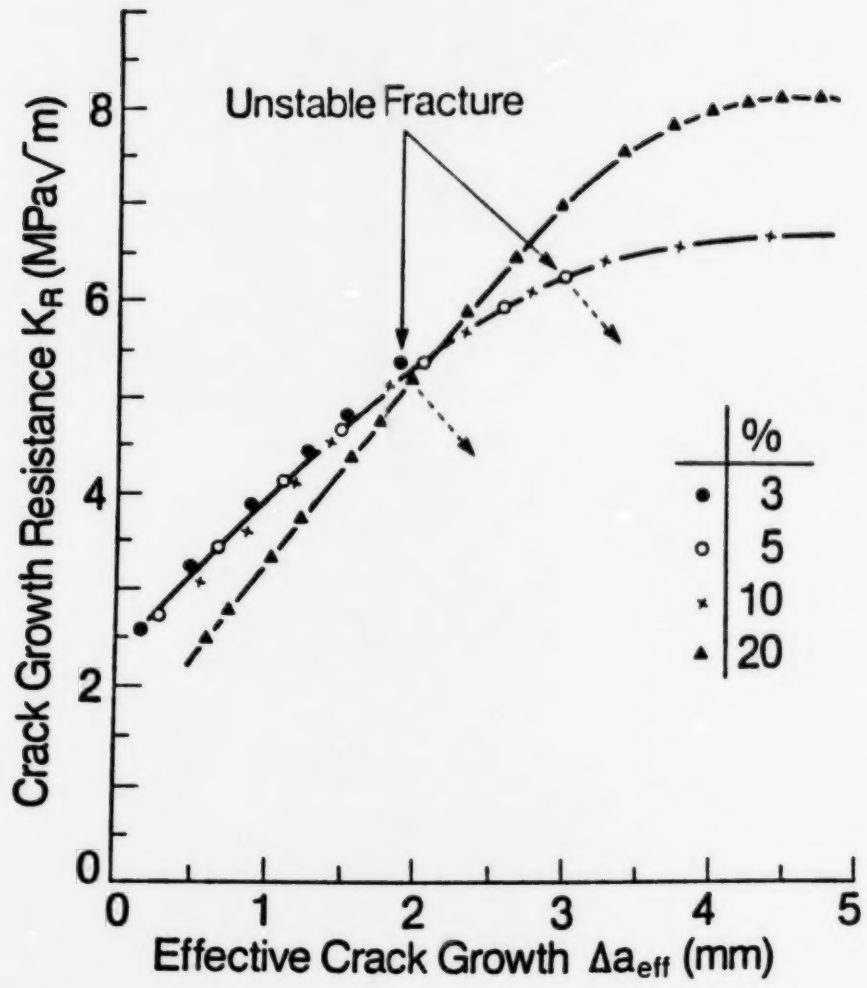

VU-KHANH Fig. 13

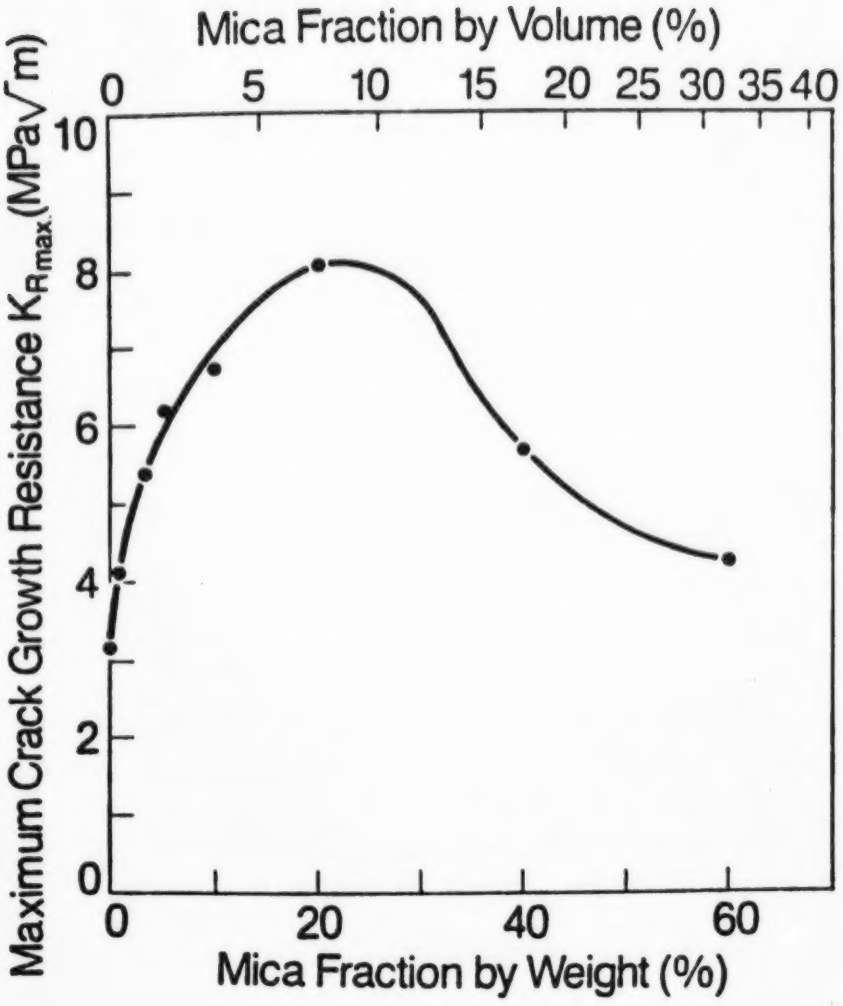

VU-KHANH Fig. 14

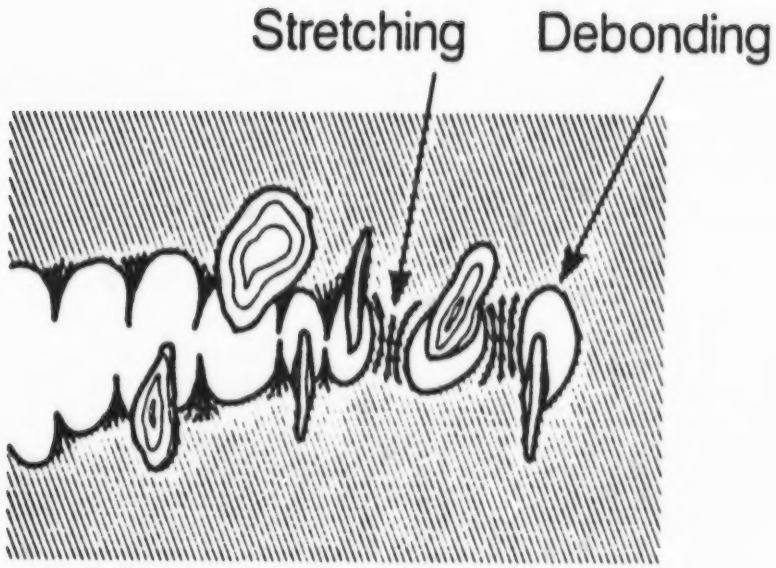

Crack Length a → Plastic Zone r_p →

VU-KHANH Fig. 15

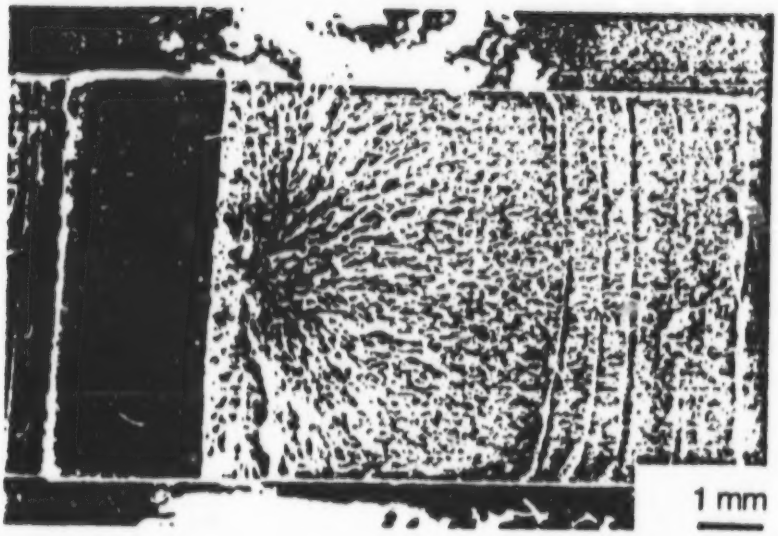

VU-KHANH Fig. 16

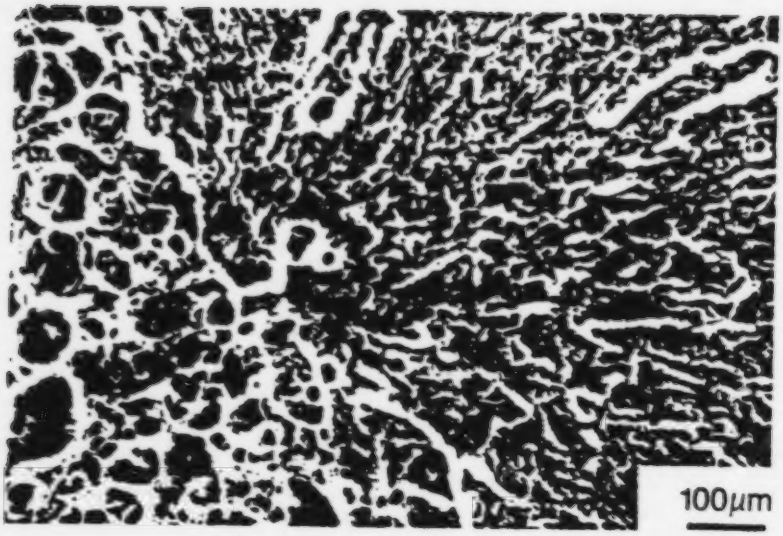

VU-KHANH Fig. 12

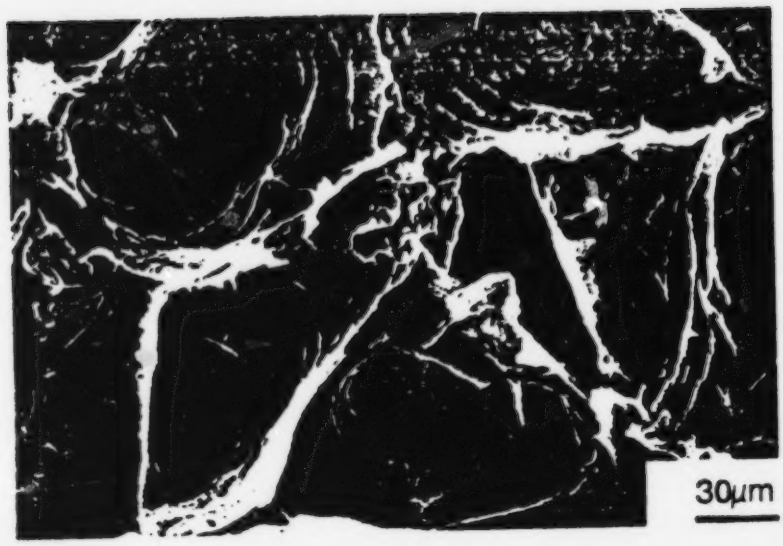

VU. KHANH Fig. 18

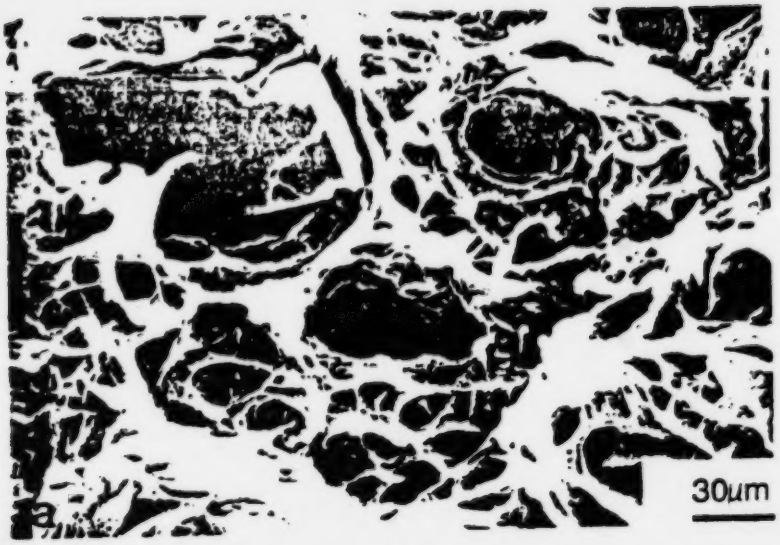

V.U. KHAN Fig. 19a

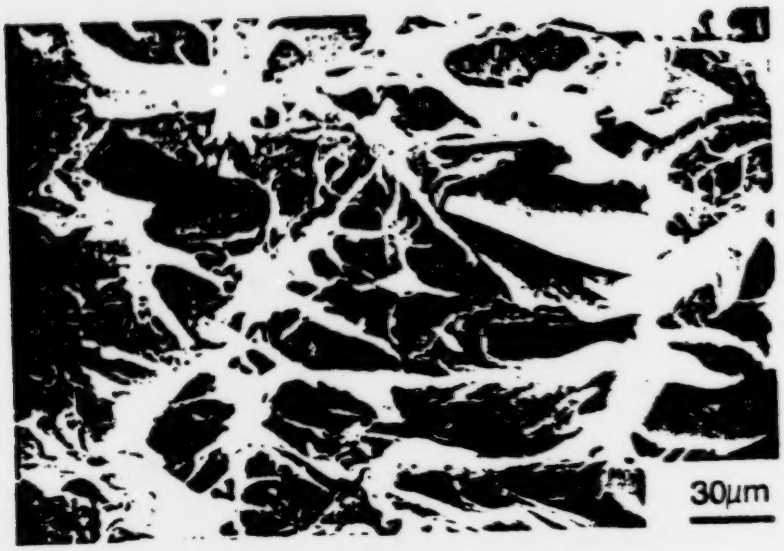

VU KHANH Fig. 19 b

VU KHANH Fig. 19c

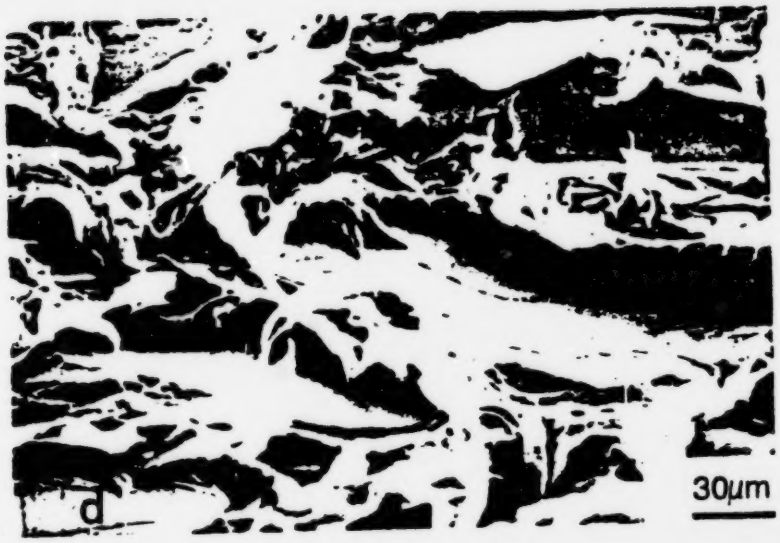

VU-KHANH Fig. 19 d

VU-KHANH Fig. 19e